Supporting Information

Chen et al. 10.1073/pnas.0904024106

SI Text

Refinement of single-particle parameters with restraints. The program FREALIGN (1) maximizes a weighted correlation coefficient (2), CC_w, to refine the x, y positions, orientations, and optionally the defocus and magnification of single-particle images. To add restraints to this refinement, we follow an approach that was described for maximum likelihood estimation of projection structures, in the limit of high signal-to-noise ratios (3). Instead of maximizing CC_w, a new score function, S, is maximized that includes information about the overall distribution of particle parameters:

$$S(\phi; \Theta) = CC_w(\phi; \Theta) + \frac{\sigma^2}{|X||A|} \ln f(\phi; \Theta). \qquad [S1]$$

ϕ is a set of parameters that need to be refined to maximize S, such as the x, y positions, orientations, defocus, and magnification. θ is a set of parameters describing the overall distribution of particle parameters. It includes, for example, the average x, y positions, the best guess of defocus from the program CTFTILT (4), and an estimate of the possible inaccuracy of the defocus. $|X|$ and $|A|$ are the norms of image X and reference A, calculated as the square root of the sum of squared pixel values. σ is the standard deviation of the noise present in image X and is given by

$$\sigma = \frac{|X - A|}{\sqrt{N}}, \qquad [S2]$$

where N is the number of pixels in image X. We assume a Gaussian distribution for the parameter distribution function, f. A Gaussian distribution will generally not correspond to the actual distribution of parameters, but it can be used as a first approximation to a restraining function if the actual distribution is not known. If there are no preferred orientations of the particles, the distribution function will only include the translational parameters x and y:

$$f_{xy}(\phi; \Theta) = \exp\left[-\frac{(x - \bar{x})^2}{2\sigma_x^2} - \frac{(y - \bar{y})^2}{2\sigma_y^2} \right]. \qquad [S3]$$

Here, ϕ includes the translational parameters x and y, and θ includes the average particle position in the dataset, x and y, and the standard deviations, σ_x and σ_y. A restraint for the image defocus can be introduced by analogy as

$$f_d(\phi; \Theta) = \exp\left[-\frac{(d - d_0)^2}{2\sigma_d^2} \right]. \qquad [S4]$$

d is the defocus assigned to a particle, and d_0 is the nominal defocus measured by the program CTFTILT. σ_d is the expected error in the nominal defocus. CTFTILT assigns defocus values by fitting the Thon rings (5) visible in power spectra of the image. To account for possible tilt in the specimen, CTFTILT also fits a defocus gradient across the image. The defocus variation is constrained to a plane, and variations due to particles positioned at different heights within the ice layer (6) are not taken into account. These smaller inaccuracies in the defocus of individual particles can be further refined using Eq. **S1** with the restraint provided by Eq. **S4**. Because of the large mass of the 7RP molecules (≈60 MD), one particle can produce sufficient signal in an image for the defocus refinement. Fig. S4 illustrates the comparison of phases between an EM particle image and its corresponding model projection. The complete restraint for translation and defocus is simply the product of the individual restraints, $f = f_{xy} f_d$. Other restraints can be added, for example for magnification and orientations. In the 7RP refinement, σ_d = 250 Å, $\sigma_x \approx \sigma_y \approx 8$ Å, and $\sigma^2/|X||A| = 0.8 \times 10^{-5}$. The refinement of particle defocus values was performed by using data between 100 Å and 9 Å resolution.

Sharpening of the Map by Using a Negative B-Factor. The B-factor of a density map can be measured using a Guinier plot (7, 8). We measured the B-factor of the icosahedrally averaged map to be ≈300 Å^2 (Fig. S5). Before nonicosahedral (13-fold) averaging, we applied the negative of this B-factor to sharpen the density map. We also applied a figure-of-merit weighting to the map (7) based on the Fourier shell correlation (FSC) curve obtained for the 13-fold averaged map (blue curve in Fig. S1). This figure-of-merit weighting attenuates the noisier structure factors at higher resolution and, therefore, avoids over amplification of these terms by the B-factor sharpening.

1. Grigorieff N (2007) FREALIGN: High-resolution refinement of single particle structures. *J Struct Biol* 157:117–125.
2. Stewart A, Grigorieff N (2004) Noise bias in the refinement of structures derived from single particles. *Ultramicroscopy* 102:67–84.
3. Sigworth FJ (1998) A maximum-likelihood approach to single-particle image refinement. *J Struct Biol* 122:328–339.
4. Mindell JA, Grigorieff N (2003) Accurate determination of local defocus and specimen tilt in electron microscopy. *J Struct Biol* 142:334–347.
5. Thon F (1966) On the relationship between phase contrast and defocus in electron microscopy. *Zeitschrift für Naturforschung A* 21:476–478 (in German).
6. van Heel M, et al. (2000) Single-particle electron cryo-microscopy: Towards atomic resolution. *Quart Rev Biophys* 33:307–369.
7. Rosenthal PB, Henderson R (2003) Optimal determination of particle orientation, absolute hand, and contrast loss in single-particle electron cryomicroscopy. *J Mol Biol* 333:721–745.
8. Sachse C, et al. (2007) High-resolution electron microscopy of helical specimens: A fresh look at tobacco mosaic virus. *J Mol Biol* 371:812–835.

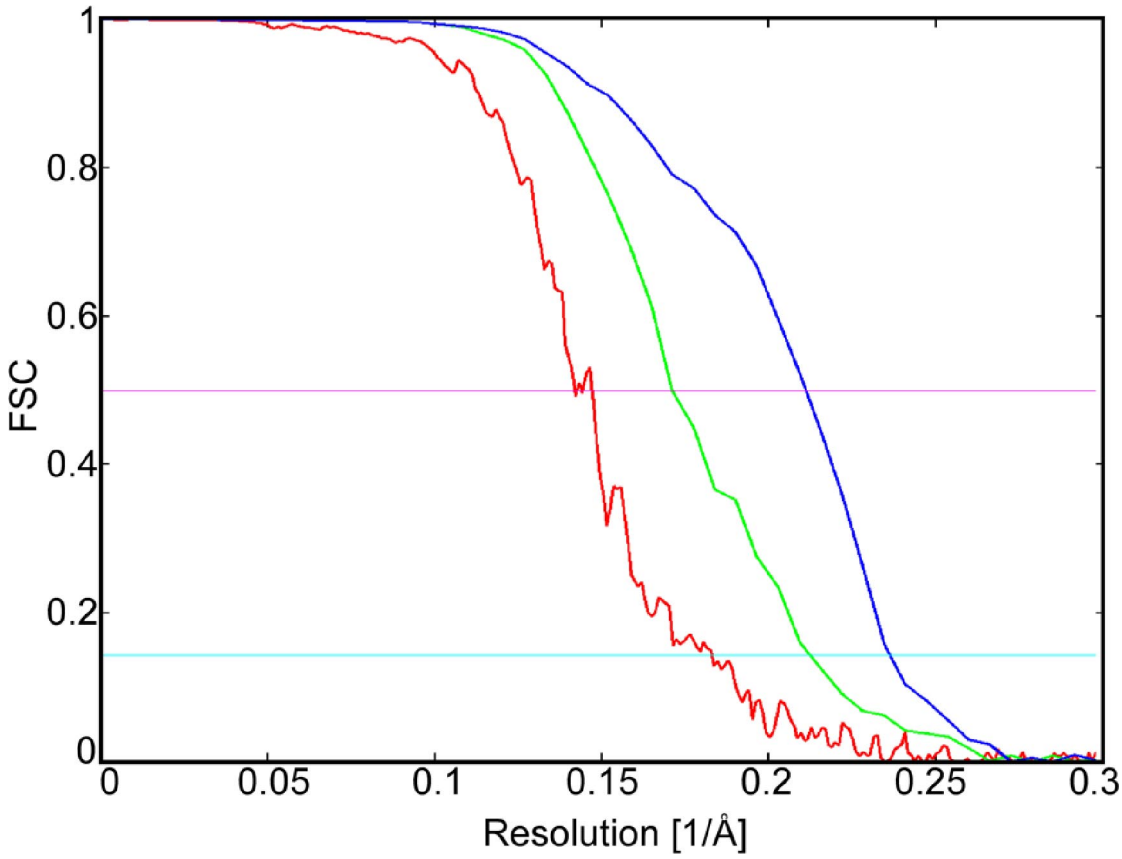

Fig. S1. FSC curves for structures at different stages of data processing. The red line shows FSC for the icosahedrally averaged density map. The green line shows FSC for the density map after additional 13-fold local averaging. The blue line shows FSC for the density map after 13-fold local averaging and additional defocus refinement of individual particles. There is noticeable improvement in the FSC between 6 Å and 4 Å.

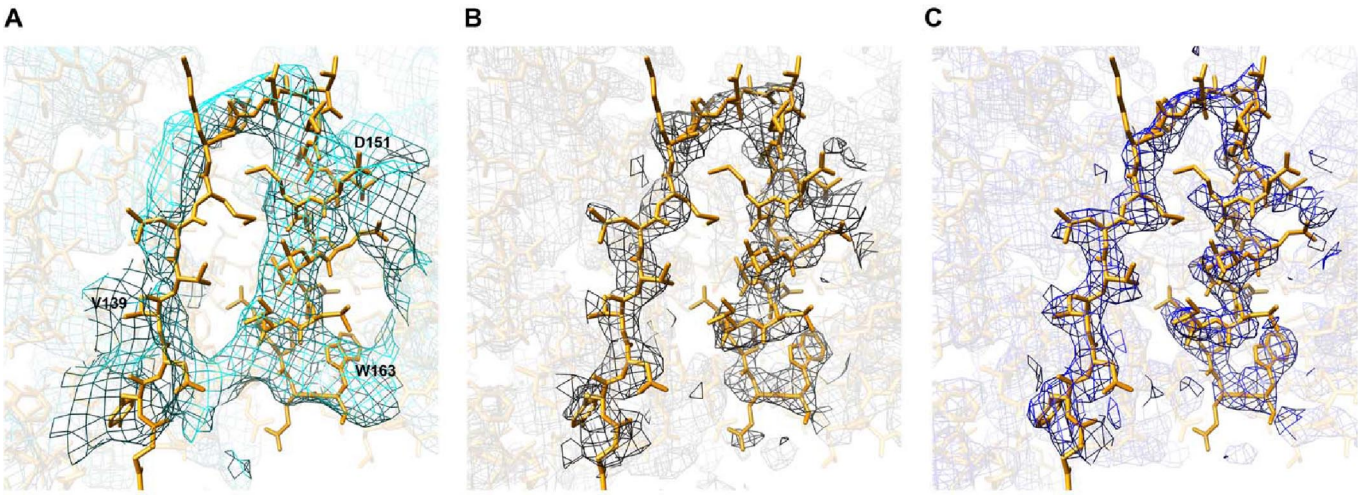

Fig. S2. Improvement of density at different stages of data processing. (*A*) Icosahedrally averaged density map with a resolution of ≈6 Å as measured by the FSC (5.5 Å at FSC = 0.143, 6.8 Å at FSC = 0.5; see Fig. S1). (*B*) Density map after additional 13-fold local averaging, at a resolution of ≈5 Å (4.5 Å at FSC = 0.143, 5.7 Å at FSC = 0.5; see Fig. S1). (*C*) Density map after 13-fold local averaging and additional defocus refinement of individual particles. The resolution improved to ≈4 Å (4.2 Å at FSC = 0.143, 4.5 Å at FSC = 0.5; see Fig. S1), and improvements in the density were also visible. The structure-map density correlation improved slightly from 0.623 in *B* to 0.671 in *C*.

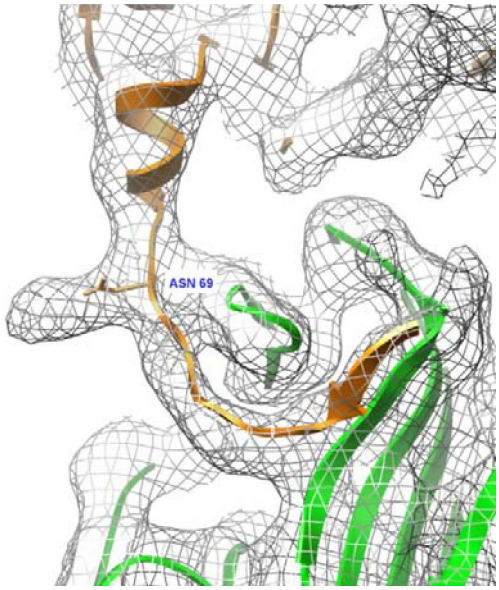

Fig. S3. Cryo-EM density filtered at 5 Å resolution. At this resolution, there is strong contrast for the density corresponding to the glycan at Asn-69.

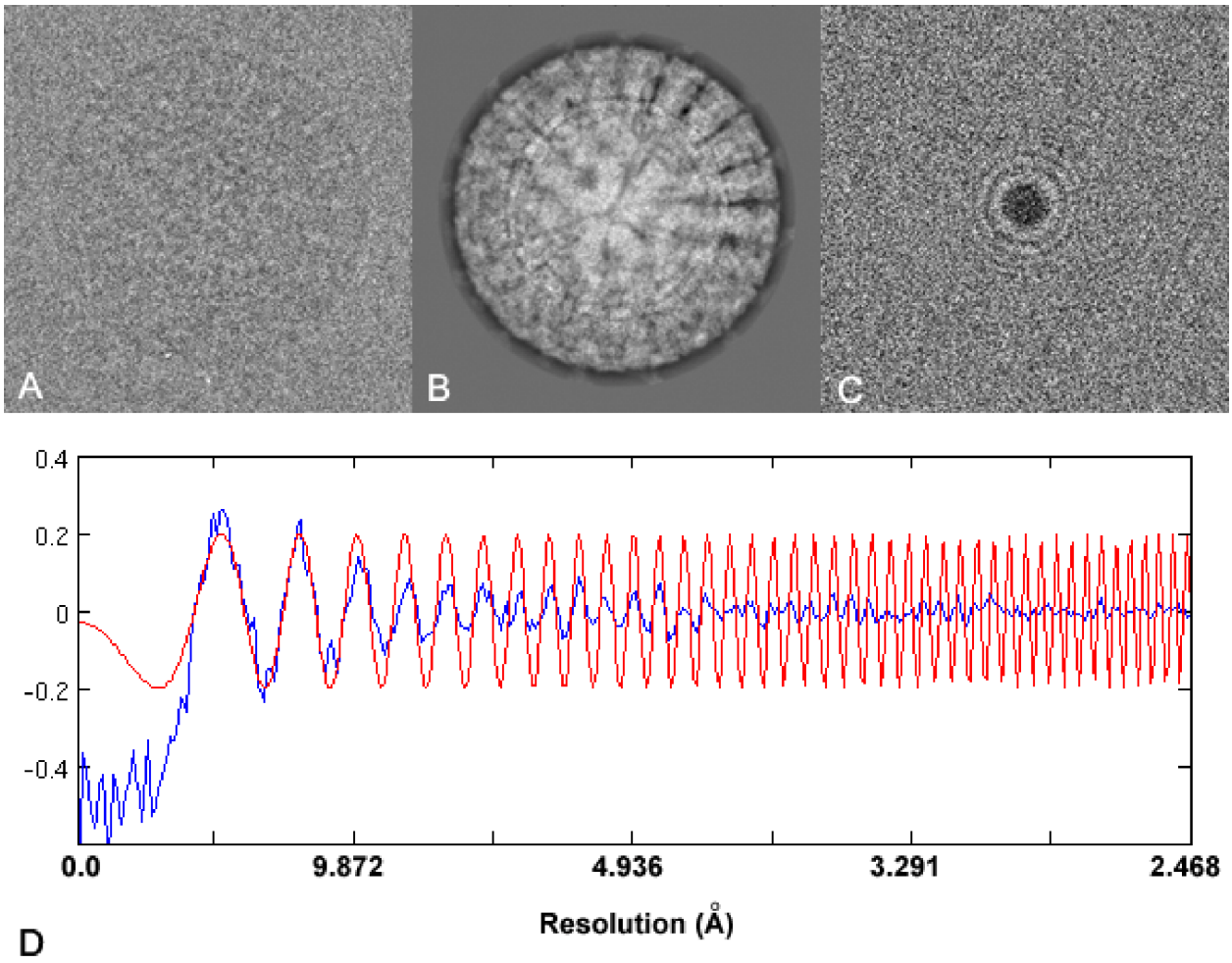

Fig. S4. Defocus refinement. (*A* and *B*) Phase-comparison between an EM particle image (*A*) and the corresponding model projection (*B*). The opposite image contrast between *A* and *B* is due to the contrast transfer function (CTF) phase flipping. The cosine of the phase difference is visualized in *C* and oscillates between in-phase (white) and out-of-phase (dark), displaying a Thon-ring pattern that can be used to fine-tune the defocus parameters. (*D*) A rotationally averaged plot (blue), overlaid by the CTF (red) using the refined defocus parameters is shown. The oscillations indicating the phase differences agree with the CTF oscillations out to ≈4.5-Å resolution, indicating sufficient signal for defocus refinement.

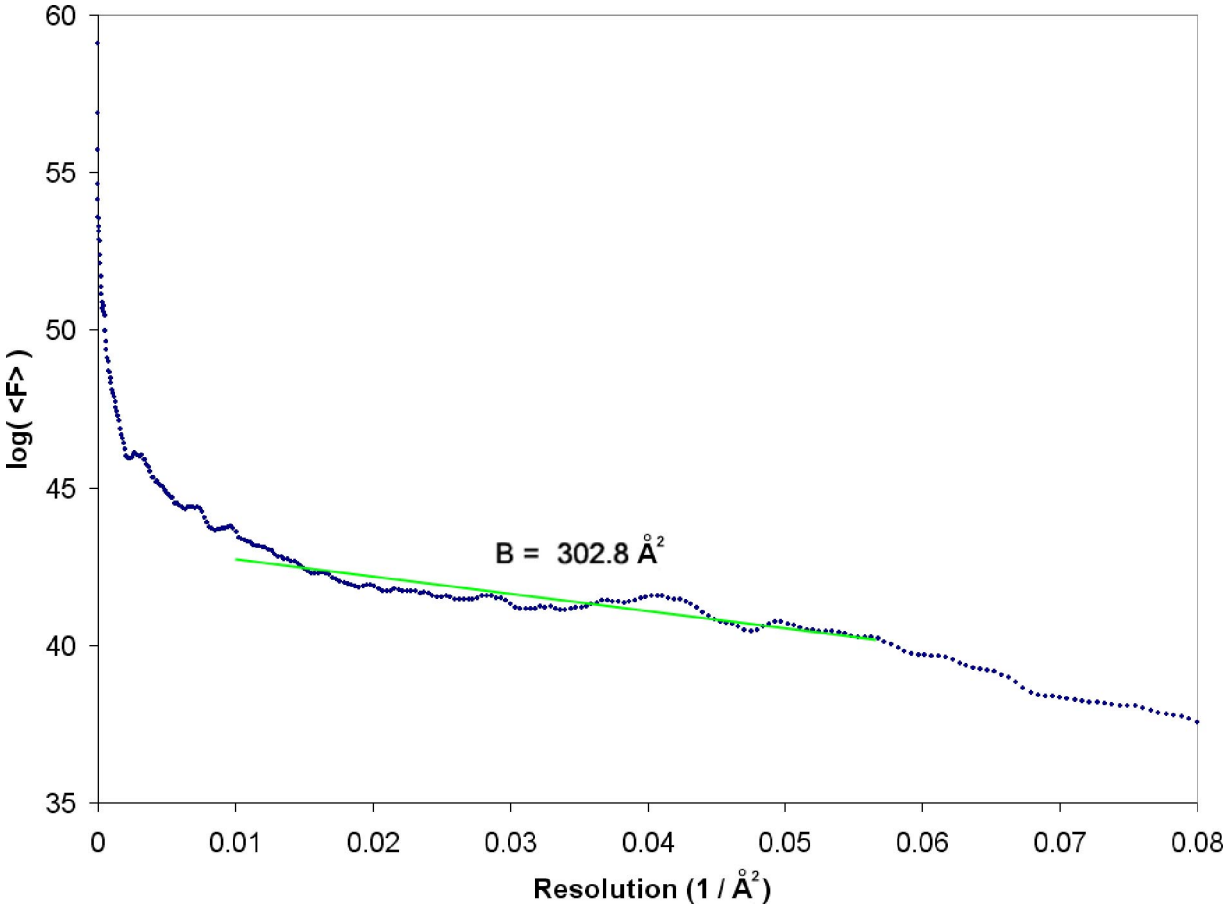

Fig. S5. B-factor sharpening of the density map. The Guinier plot for the icosahedrally averaged structure shows a slope that was fitted between 10 Å and 4.2 Å with a B-factor of ≈300 Å^2. The fit was performed before figure-of-merit weighting.

Table S1. VP6–VP7 contact in the 7RP particle

	VP6	VP7
van der Waals	Pro313	Pro279, Thr281
H-bonding	Asn310	Gln305
β-strand	Asn167–Ser163	Pro58–Ser62